Palaeogeography, Palaeoclimatology, Palaeoecology xxx (2016) xxx–xxx

Contents lists available at ScienceDirect

Palaeogeography, Palaeoclimatology, Palaeoecology

journal homepage: www.elsevier.com/locate/palaeo

Modeling climatic effects of carbon dioxide emissions from Deccan Traps Volcanic Eruptions around the Cretaceous–Paleogene boundary

Thomas S. Tobin [a,*], Cecilia M. Bitz [b], David Archer [c]

[a] University of Alabama, Geological Sciences, United States
[b] University of Washington, Atmospheric Sciences, United States
[c] University of Chicago, Geophysical Sciences, United States

ARTICLE INFO

Article history:
Received 26 January 2016
Received in revised form 12 May 2016
Accepted 25 May 2016
Available online xxxx

Keywords:
Deccan
Model
Cretaceous
K–Pg
Paleogene
Climate

ABSTRACT

Warming events observed in paleotemperature proxy records within 500 ka of the Cretaceous–Paleogene (K–Pg) boundary have often been attributed to atmospheric CO_2 increases due to Deccan Traps Flood Volcanism. Currently, there is uncertainty in the size, nature, and timing of the Deccan eruptions, all of which lead to uncertainty in the likely climatic effects. Modeling the impact of Deccan Traps eruption on climate is complicated by the discrepancy between the lifetimes of emitted gasses and the length of the total eruptive sequence. Though SO_2 emissions can have important climatic effects, the short atmospheric lifetime of SO_2 and resulting aerosols means these effects are unlikely to be recognized in the proxy record. Here we focus on the CO_2 emissions, and attempt to match paleotemperature proxy records with plausible emissions scenarios. We also test the relevance for climate of the number, length, and arrangement (e.g., increasing or decreasing size) of individual eruptions as well as the total duration and size of the overall eruptive sequence. We find that the number and length of individual eruptions are largely unimportant to CO_2 based climate effects, but that the pattern and duration of eruption have measureable effects. Unsurprisingly, the total emitted CO_2 from the Deccan Traps exerts a strong control on climatic effects, and better constraints on the volume of emitted gas are necessary. At the high end of the uncertainty range, the Deccan Traps eruptions are capable of generating warming events recorded in the proxy record, but rates of silicate weathering above modern rates are necessary to draw down CO_2 in accordance with those records.

1. Introduction

The end-Cretaceous mass extinction is generally thought to be the consequence of a large bolide impact (Schulte et al., 2010) that effectively defines the Cretaceous–Paleogene (K–Pg) boundary (Molina et al., 2006). However, climatic impacts from Deccan Traps flood volcanism have also been implicated as a primary or aggravating contributor to the mass extinction (Tobin et al., 2012; Keller, 2014; Tobin et al., 2014; Wilson, 2014). The possible temporal correspondence between the Deccan Traps and extinction has been the primary driver of this hypothesis, and similar correlations between large igneous provinces and mass extinctions have been noted throughout the Phanerozoic (Courtillot and Renne, 2003; Bond and Wignall, 2014). The largest mass extinctions are global events, and to have global biotic effects, flood volcanism must alter atmospheric chemistry and/or climate in ways that spread globally as well. The primary means through which volcanism alters atmospheric chemistry is the release of carbon dioxide (CO_2) and sulfur dioxide (SO_2), though the release of halogens may also generate acid rain, potentially globally (Font et al., 2014).

Carbon dioxide and SO_2 are generally thought to have competing climatic effects — CO_2 warms the planet through increased absorption of Earth's radiated heat (increased greenhouse effect), while SO_2 forms aerosols that block incoming solar radiation, cooling the planet (Bond and Wignall, 2014). Because the atmospheric lifetimes of these constituents are very different: the cooling effects from volcanism essentially end a few years after the eruption, and may be reduced in flood basalt eruptions when compared with more explosive eruptions (Schmidt et al., 2016), while the warming effects of CO_2 can persist well beyond (thousands of years) the initial release of the gas. In many studies of the potential atmospheric impact of flood volcanic volatile release, it is assumed that cooling from SO_2-derived volcanic aerosols is the more likely candidate to have biological consequences, as even an individual flow is capable of generating substantial global cooling (Self et al., 2014; Self et al., 2015). While these cooling events could be the primary means through which flood basalts affect global biota, the duration of these cooling events makes it highly unlikely that they would ever have been detectable and confirmed in the stratigraphic record. It is also possible that SO_2 leads to substantial acidification and related biotic effects, but Schmidt et al. (2016) suggest this is unlikely.

* Corresponding author at: University of Alabama, Geological Sciences, 201 7th Ave, 35487 Tuscaloosa, AL, United States.
E-mail addresses: ttobin@ua.edu (T.S. Tobin), bitz@uw.edu (C.M. Bitz), d-archer@uchicago.edu (D. Archer).

http://dx.doi.org/10.1016/j.palaeo.2016.05.028
0031-0182/

The longer duration of CO_2 related warming is likely detectable in the fossil record. Paleotemperature data from periods of flood basalt eruption are mixed, but it appears that most large continental flood basalts are associated with global warming (Bond and Wignall, 2014). For the end Cretaceous mass extinction, a warming event during the last ~350 ka (though see discussion of timeframe below) of the Cretaceous has often been linked with the Deccan Traps volcanism (Li and Keller, 1998; MacLeod et al., 2005; Tobin et al., 2012). The CO_2 release from an individual eruption is almost certainly too small to have a significant impact on atmospheric CO_2 levels, and this observation, combined with the spacing between eruptions, has been used to argue that volcanic CO_2 from flood basalts cannot generate substantial warming (Self et al., 2006). Modeling of modern emission scenarios suggest that 20–25% of a suddenly emitted CO_2 perturbation will persist for over 10 ka (Archer et al., 2009), a long enough period that CO_2 could potentially accumulate in the atmosphere between eruptions in a flood basalt eruptive period where average spacing is likely on the order of 1 ka (Self et al., 2014).

2. Deccan Traps and warming

Below we investigate whether the size and episodic nature of Deccan CO_2 emissions is sufficient to generate warming that has been observed using paleotemperature proxies. Many authors have attributed warming near the K–Pg boundary to Deccan Traps CO_2 emissions based on plausible contemporaneity (e.g. Li and Keller, 1998; Barrera and Savin, 1999; Wilf et al., 2003; Tobin et al., 2012), but there are few ways to prove a causal connection. Most of the Deccan Traps emissions are emitted during magnetochron C29R, an interval lasting roughly 700 ka spanning the K–Pg boundary (Ogg, 2012 and references therein). Recent and ongoing research into the timing of Deccan emissions could potentially rule out a causal connection (Renne et al., 2015; Richards et al., 2015), but temporal correspondence will always be insufficient in proving causality. At present, it is unlikely that definitive proof of causality can be obtained from the geologic record, but climate modeling based on constraints of eruptive size and duration can provide an additional test of a Deccan — warming link.

Previous attempts at modeling warming from Deccan Traps flood volcanism have produced mixed results. Caldeira and Rampino (1990a) found little to no measurable impact from possible Deccan volcanism, though they also found potential warming below 2 °C for what they considered unreasonably high levels of CO_2 emissions (Caldeira and Rampino, 1990b). Dessert et al. (2001) modeled a more substantial warming, up to 4 °C, but they used CO_2 emissions that are likely too high (see discussion below). Recent attempts to model the combined contributions of SO_2 and CO_2 emissions suggest that reduced warming from individual eruptions would have suppressed weathering and CO_2 drawdown, increasing the accumulation of CO_2 in the atmosphere and consequent warming (Mussard et al., 2014). Unlike the previous models, their model simulated individual eruptions, rather than modeling a single increased rate of emissions for the entire period of Deccan eruptions. However, due to the complexity of their hybrid model, they did not test how varying eruptive duration, length and pattern affected their results. We employ a simpler model that allows a more complete testing of these parameters, but focused exclusively on CO_2 emissions.

3. Model details

We use a modified version of the GEOCYC model (Archer et al., 2009), which originally was based on previous GEOCARB models developed by Berner (Berner, 1994; Berner and Kothavala, 2001). This model iterates over a user-defined time step and tracks carbon through globally-averaged atmospheric and oceanic reservoirs, with the oceanic reservoir partitioned into dissolved inorganic carbon species ($CO_{2\ (aq)}$, HCO_3^-, and CO_3^{2-}). Carbon is removed from the atmosphere through silicate and carbonate weathering and added through volcanic emissions. Carbon is removed from the ocean through carbonate burial and added through weathering, with gas exchange moving carbon between the ocean and atmospheric reservoirs. Atmospheric CO_2 concentration (or level) is converted to atmospheric temperature using a climate sensitivity set to 3 °C per doubling of CO_2, likely on the low end of Cretaceous climate sensitivity estimates (Breecker et al., 2010; Royer, 2010). The atmosphere temperature equilibrates instantly with CO_2 level, while the ocean temperature has a 1 ka relaxation rate with respect to the atmosphere. The ocean temperature primarily affects gas solubility and exchange. As this model is functionally similar to its predecessors, we refrain from a detailed description here, but provide a commented MATLAB script in the Supplemental material for others to use. Archer et al. (2009) demonstrated that this model compares favorably in terms of CO_2 drawdown with other more complex models in modern simulations, particularly over geologically relevant time scales. GEOCYC was designed to test modern day climate scenarios, and used pre-industrial conditions as a baseline, as did the model of Mussard et al. (2014).

3.1. Model modifications

Several modifications to GEOCYC were made to match more closely with Cretaceous climatic conditions prior to the eruption of the Deccan Traps and are detailed in the MATLAB climate code (see Supplemental material). We altered the percentage of exposed land area, mean continental latitude, and a parameter relating global river runoff to changes in global mean temperature. The sensitivity of the model to these parameters is outlined below (Section 4.1). The solar constant was reduced by a small fraction (~0.4% — Feulner, 2012) to replicate the slightly weaker sun at 66 Ma, but the effect was negligible. In each model run, we prescribe a CO_2 emission scenario representative of the Deccan trap eruptions, added to a background CO_2 level. Because CO_2 drawdown and temperature scale non-linearly with CO_2 level the climate response depends on both the background CO_2 level and the Decan trap CO_2 emissions scenario. It is important to initiate our Deccan emission tests at background CO_2 levels (and hence temperatures) similar to those present at the end of the Cretaceous. We tuned background CO_2 levels to 450 ppm (Beerling et al., 2002) by altering background CO_2 emission rates to a higher value, a plausible change given the faster seafloor spreading rates in the Cretaceous (Seton et al., 2009). The model was allowed to stabilize at these new conditions during a "spin-up" period, resulting in a global air temperature of 17 °C prior to the simulated eruption of Deccan Traps. The time step in the original model was 50 years, and here we reduced it to 10 years, a necessary change to test shorter duration eruptions. Nonetheless, using MATLAB, the model completes a run of over one million simulation years in under a minute on a modern desktop computer. Tests were completed for shorter time steps, 1 year or less, with no discernible difference in results.

3.2. Eruption scenarios

Previous studies, with the exception of Mussard et al. (2014), have generally assumed continuous eruption of Deccan basalts over the entire eruptive period. In our case we simulate eruptions by increasing the rates of CO_2 emission above background for discrete time periods that can vary in their size, pattern, duration, and spacing (see Section 4.2 below), allowing us to test whether the episodic nature of these eruptions is important to their climatic effects. We can alter these eruptive parameters independently of each other and the total CO_2 emissions. The major areas of uncertainty in determining the total CO_2 emitted are the volatile content percentage of the lavas and the original total volume of eruptive material (see Section 4.2 below). We input total CO_2 emission into the model that are calculated from lava quantity and volatile percentage, or use previously calculated estimates of emitted CO_2 (see below).

Please cite this article as: Tobin, T.S., et al., Modeling climatic effects of carbon dioxide emissions from Deccan Traps Volcanic Eruptions around the Cretaceous–Paleogene boundar..., Palaeogeogr. Palaeoclimatol. Palaeoecol. (2016), http://dx.doi.org/10.1016/j.palaeo.2016.05.028

4. Modeling results

We tested several variables that alter the pattern of CO_2 emissions (Fig. 1), which we define here for greater clarity. The *eruptive sequence* is the total period over which CO_2 is emitted from Deccan eruptions, including hiatuses. An *eruption* is a single, mostly continuous, eruptive event leading to a single lava flow. We can alter the *length* (in years) of single eruption, and/or the *duration* (in years) of the eruptive sequence. Additionally the *number*, *spacing*, and *pattern* (see Section 4.2 below) of eruptions can also be altered, as can the *total* CO_2 emitted over the whole eruptive sequence. Given current understanding of the Deccan Traps, we believe the best estimates for the various parameters tested above are: a total amount of emitted CO_2 of 4.14×10^{17} mol, based on lava volume estimates from Jay and Widdowson (2008) and volatile release from Self et al. (2006); total eruptive sequence of 400 ka based on constraint of Deccan emissions to C29R and early C29N (Schoene et al., 2015) and a conservative (long) estimate C29R duration of 710 ka (Ogg, 2012); number of eruptions — 250; length of individual eruptions — 20 years (Self et al., 2015); and a pattern of equal sized eruptions throughout the eruptive sequence, given little other knowledge of eruption patterns at present. For most results displayed below, we chose to use a much reduced number of eruptions (20) and increased length of eruption (5 ka), as they facilitate visual interpretation of output data, and we later demonstrate (Section 4.2) that an increased eruption length and decreased number of eruptions are inconsequential to our final results. We continued to use the likely values for total emitted CO_2, eruptive sequence duration and flow pattern for all the model tests in Section 4, unless the variable in question was being tested.

4.1. Significant Cretaceous adjustments

Here we examine the model sensitivity to modifications that mimic Cretaceous geographic and environmental conditions (i.e., those not associated with specific Deccan volcanism related changes outlined in Section 4.2). Note that in some of these scenarios we modified the background CO_2 emission rate to generate similar initial conditions prior to a simulated eruption.

4.1.1. Mean latitude of continents

The location of subaerially exposed continental landmasses will affect weathering rates, as weathering rates at tropical latitudes are higher than near the poles. A greater area of continents near the equator will result in globally higher weathering rates and faster drawdown of CO_2. The modern mean latitude used for the standard GEOCYC model is 30°N due to the current bias of landmass in the northern hemisphere, though the model does not differentiate between a northern or southern hemisphere bias. The land was more evenly distributed hemispherically in the Late Cretaceous, based on image analysis of equal area projections from Blakey (2012), so we test the sensitivity to the mean-latitude. For our sensitivity tests we use a scenario of CO_2 emissions from a series of 250 individual Deccan-like eruptions of equal magnitude. Because the response to such an eruption scenario is sensitive to the initial CO_2 atmospheric concentration, the background CO_2 emission rate was varied (respectively, mean latitude = 30°, 20°, 10°, 0°; moles of CO_2/year = 7.43×10^{12}, 8.03×10^{12}, 8.41×10^{12}, 8.55×10^{12}) so that each model run equilibrated to the same atmospheric concentration prior to the initiation of the eruptive sequence. However, with modification of the background emissions, the response to the eruption scenario had little dependence on mean latitude (Fig. 2), though the effect is in the expected direction.

4.1.2. Total land area

A portion of the CO_2 exiting the atmosphere comes from chemical weathering of exposed land area, and a greater extent of exposed land area will result in an increased rate of CO_2 draw down. Due to higher sea levels during the Cretaceous, less land area was exposed than modern conditions. Using the same image analysis described above we found that Late Cretaceous land area was 95% of today. The total land area exposed above sea level in this model is expressed as multiplier on the modern land area. Like continental mean latitude, the model is sensitive to this value in the spin-up stage (respectively, land fraction = 0.95, 1.00, 1.05; moles of CO_2/year = 8.41×10^{12}, 8.87×10^{12}, 9.33×10^{12}), but not significantly so in the simulation of Deccan-like eruption. Less exposed land area slows weathering rates, so this modification leads to increased CO_2 buildup and higher temperatures when lowered, but again by minor amounts (Fig. 3). This change acts in the opposite direction to the mean latitude adjustment (above) with a similar (though not identical) magnitude.

4.1.3. River runoff

The volume of river runoff affects the strength of chemical weathering and effectiveness of transport of weathering products to the ocean. The response of river runoff to changes in temperature is non-linear, and is modeled by Berner and Kothavala (2001) as a bimodal process. When there are substantial continental ice sheets present, river runoff changes more quickly with changes in temperature due to formation and melting of glacial ice, while in periods without major glaciation, the change is more subdued. A coefficient describing this relationship was modified from a modern icehouse value (0.045) to a hothouse condition (0.025). This change leads to increased atmosphere pCO_2 values relative to icehouse conditions, all else being

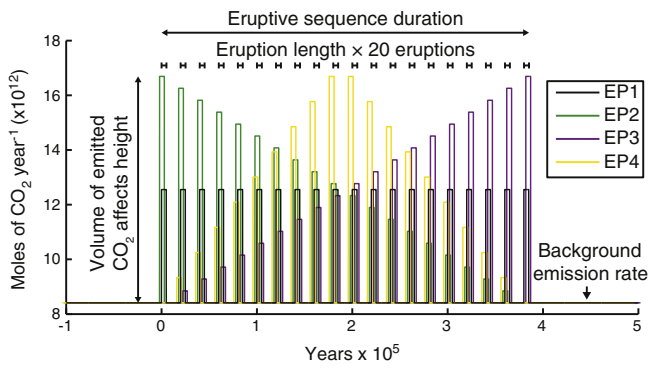

Fig. 1. Example simulated emission scenarios and definition of terms used throughout this paper. Different eruptive patterns: (EP1) periodic but equal sized eruptions; (EP2) periodic eruptions that ramp down from an initial peak; (EP3) periodic eruptions that ramp up to a final peak; (EP4) periodic eruptions that ramp up and back down. Patterns are slightly time shifted from each other to better illustrate their shapes.

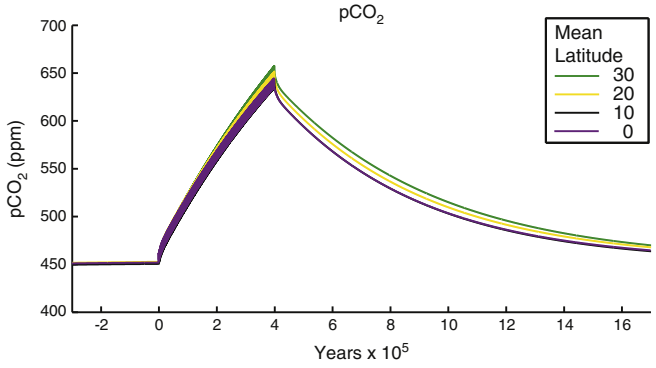

Fig. 2. Test of model response in globally averaged pCO_2 to changes in the mean latitude of continental land area. Background CO_2 levels are held constant by varying background CO_2 emission rates (see text), and an eruptive sequence duration lasting 400 ka, releasing 4.14×10^{17} mol of CO_2 in 250 eruptions lasting 20 years each is added to the background. Chemical weathering is lower at higher latitudes, so CO_2 drawdown is lower when continents are located in more polar locations.

Please cite this article as: Tobin, T.S., et al., Modeling climatic effects of carbon dioxide emissions from Deccan Traps Volcanic Eruptions around the Cretaceous–Paleogene boundar..., Palaeogeogr. Palaeoclimatol. Palaeoecol. (2016), http://dx.doi.org/10.1016/j.palaeo.2016.05.028

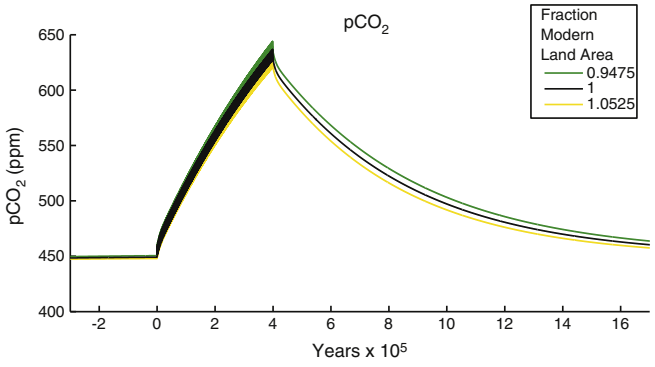

Fig. 3. Test of model sensitivity to the amount of subaerially exposed land area, expressed as a fraction of modern area. Greater surface exposure increases the rate of chemical weathering and CO_2 drawdown. The background CO_2 emissions for each run are tuned to create equal pCO_2 values prior to simulation of eruption sequence releasing 4.14×10^{17} mol of CO_2 over 400 ka in 250 separate eruptions lasting 20 years each.

equal. However, from the same initial pCO_2 level, the magnitude of the impact on volcanic emission simulations is fairly minor (Fig. 4).

4.1.4. Background CO_2 levels

As described above, we tuned the background CO_2 level prior to the eruptions to 450 ppm to correspond with proxy records. Various authors have proposed a range of values for CO_2 from as low as 375 (Royer, 2003) to 540 ppm (Beerling et al., 2009) with possible error bounds extending from 340 to 785 ppm. Though partially based on the previous work, other recent time series of CO_2 proxies have accepted similar values for the K–Pg time period, with values between 400 and 500 ppm and uncertainties ranging from 350 to 800 ppm (Breecker et al., 2010; Beerling and Royer, 2011). The non-linearity of the temperature — CO_2 relationship results in larger increases in temperature for the same Deccan simulation at lower starting CO_2 values, though the affect is moderated by the long duration of emission combined with the increased ability of a less saturated ocean to absorb CO_2 when initial pCO_2 is lower (Fig. 5).

4.2. CO_2 emission scenario sensitivity

CO_2 emission from flood basalt volcanism is commonly disregarded as inconsequential due to the relatively small size of each individual eruptions and their episodic nature, which could allow CO_2 levels to return to background before the subsequent eruption (Self et al., 2006). We tested the importance of total emitted CO_2 (related directly to total lava volume emitted), duration of total eruption sequence, number of individual eruptions, the length of individual eruptions, and the pattern of eruption size. We find the primary controls on climate response are ultimately the total CO_2 emissions and duration of the entire eruptive sequence, but we explore each variable independently below. Starting conditions are as described above, except when testing the specific variable.

4.2.1. Number of eruptions

It is unlikely that the exact number of eruptions in the Deccan Traps sequence will ever be known, but it is probably on the order of 100 (Chenet et al., 2007; Chenet et al., 2008; Jay and Widdowson, 2008; Chenet et al., 2009; Jay et al., 2009). We tested a range of possibilities, from very low (20) to the upper high end of possibilities (1000). Fig. 6 shows the model results for these variations, with every other value held constant. The results show clearly that number of eruptions is not important on a long time scale, at the end of the eruptive sequence every scenario results in effectively identical CO_2 levels and air temperatures. Limiting the number of eruptions generates short term spikes in CO_2 as a result of compressing the total CO_2 emissions to a shorter total emissions period.

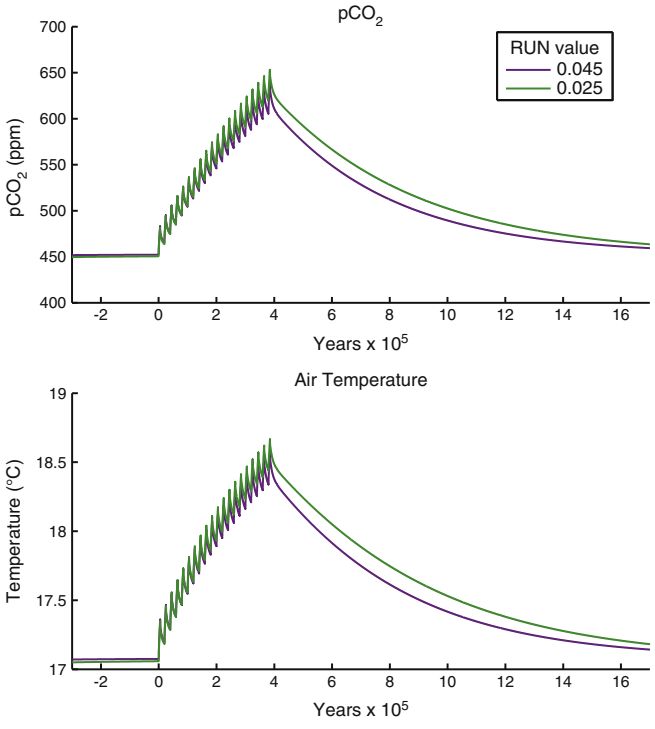

Fig. 4. Test of model sensitivity to the RUN parameter in atmospheric pCO_2 and temperature (below), which controls the relationship between temperature and global river runoff. Berner and Kothavala (2001) distinguished between icehouse conditions (0.045) and hothouse conditions (0.025). The background CO_2 emissions for each run are tuned to create equal pCO_2 values prior to simulation of eruption sequence releasing 4.14×10^{17} mol of CO_2 over 400 ka in 20 separate 5 ka eruptions.

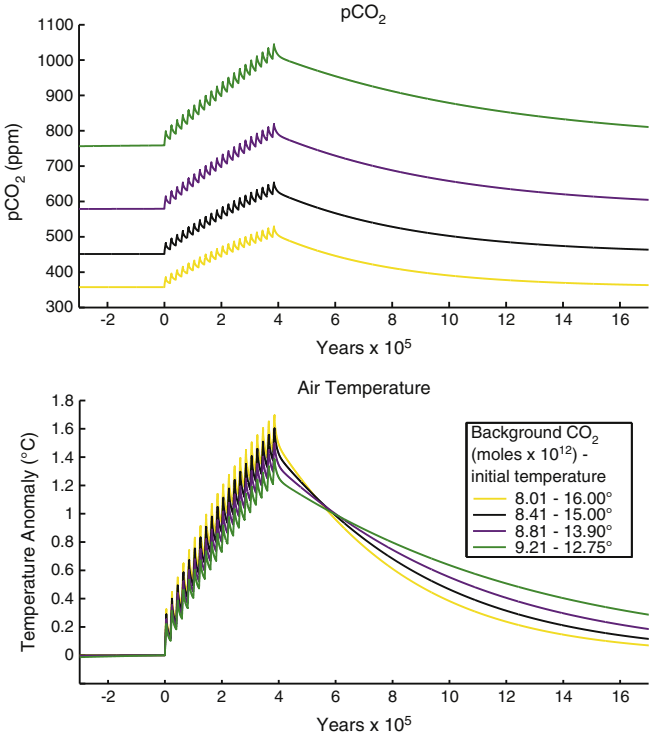

Fig. 5. Testing the effects of background CO_2 levels prior to Deccan Traps emissions on identical Deccan-like emissions. Different background CO_2 emission rates and starting temperatures were used to create initial conditions with the same temperature but different pCO_2 values. Higher initial CO_2 levels resulted in lower magnitude warming events.

Please cite this article as: Tobin, T.S., et al., Modeling climatic effects of carbon dioxide emissions from Deccan Traps Volcanic Eruptions around the Cretaceous–Paleogene boundar..., Palaeogeogr. Palaeoclimatol. Palaeoecol. (2016), http://dx.doi.org/10.1016/j.palaeo.2016.05.028

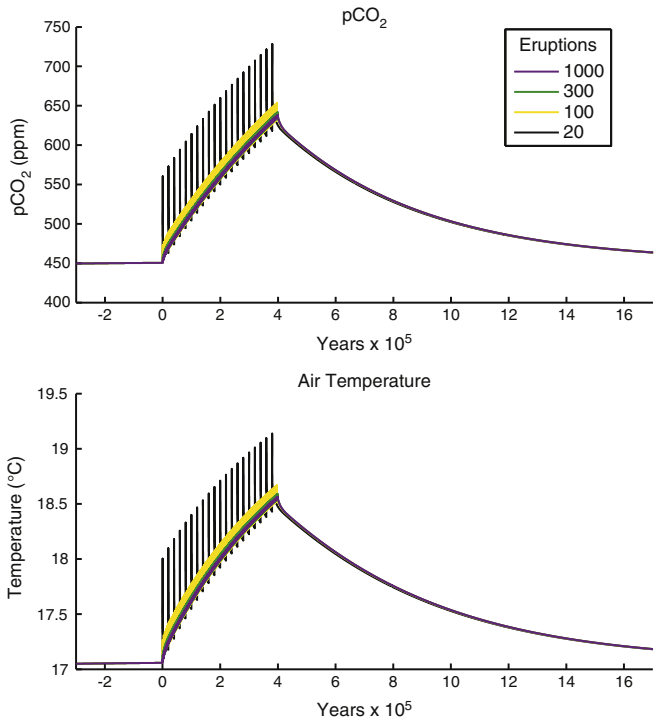

Fig. 6. Test of the effects of varying the number of individual eruptions comprising the total Deccan eruptive sequence. Because the eruptive sequence duration, total amount of CO emitted, and eruption length are fixed, the CO_2 emitted in each eruption varies accordingly with the number of eruptions. For realistic numbers of eruptions (>100) there is little difference among runs.

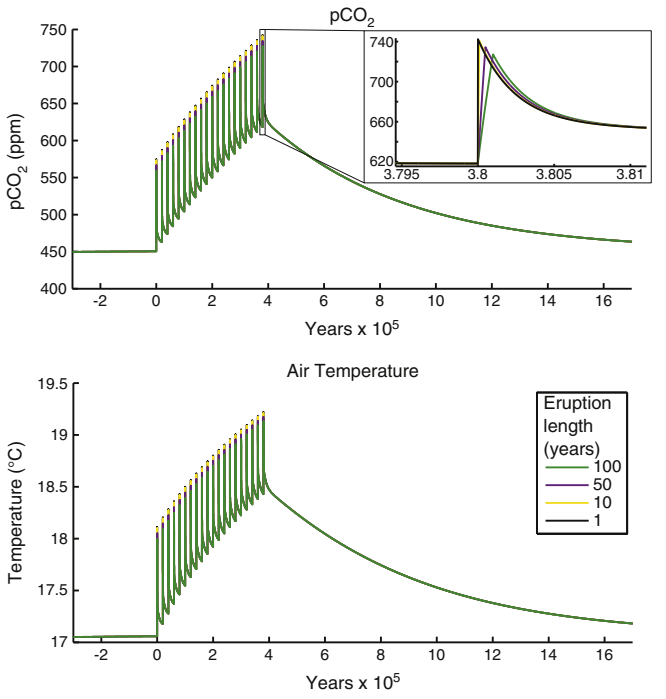

Fig. 7. Test of the effects of varying the length of individual eruptions within the Deccan sequence. Short term differences are minimal (see inset) and there is no effective difference in longer term effects.

4.2.2. Length of eruptions

The length of individual eruptions in the Deccan Traps, and other flood basalt provinces, is poorly understood. Self et al. (2014) suggest that individual eruptions are likely extruded on the order of decades, but whether or not substantial outgassing occurs throughout this whole eruption is unclear. Given these uncertainties we tested a wide range of flow length possibilities, from one year to 100 years. For testing flow lengths less than ten years the model time step (set to 10 years for most tests), must be reduced to the shortest flow length desired (in this case 1 year). The length of each flow was varied, assuming all eruptions were of equal size with continuous outgassing throughout each eruption. Individual flow length has a negligible effect on CO_2 levels or temperatures in the long (100's of ka) or short (100's or years) term (Fig. 7). For given eruptions of identical size but differing lengths, there is only a fairly small difference between the peak CO_2 level and air temperature, and the differences are quickly erased between eruptions.

4.2.3. Pattern of eruption size

At present it is unclear how continuous the eruptive sequence of the Deccan Traps was. Richards et al. (2015) suggest that the majority of the eruptive volume was erupted towards the end of the Deccan Traps sequence (most similar to EP3 below), but they acknowledge that further age dating is necessary. Renne et al. (2015) further suggest that most of the Deccan sequence was erupted in the Danian as a consequence of the Chixculub impact. Their geochronology suggests that much of the Deccan Traps was erupted post-K–Pg, but their estimates rely on interpolation to estimate age of many of the large volume flows, and the results should probably be treated as tentative pending further testing of the Ambenali and Poladpur flows. With a lack of constraining information, we tested four different emissions patterns (Fig. 1): (EP1) periodic but equal sized eruptions; (EP2) periodic eruptions that ramp down from an initial peak; (EP3) periodic eruptions that ramp up to a final peak; (EP4) periodic eruptions that ramp up and back down. The results of this test (Fig. 8) may initially be counterintuitive; the highest CO_2 level and temperature occur with more of the gas emitted later in the eruptive sequence, rather than near the beginning. EP3, has the highest peaks, while EP2, has the lowest, with EP1 and EP4 being fairly similar. While notable, these differences are likely too small to have substantial climatic or biological effects.

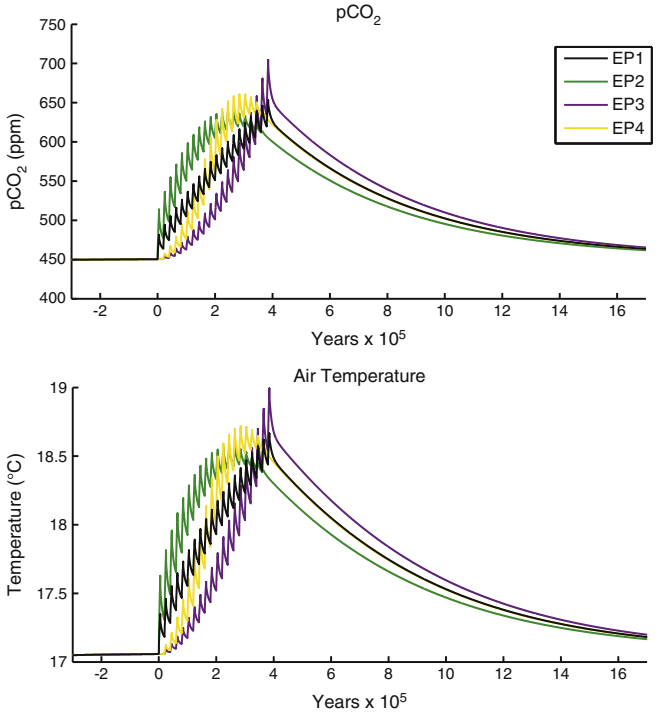

Fig. 8. Test of the effects of different eruption patterns over the total eruptive sequence. Slightly higher peak values are found with EP3 when compared with EP2.

Please cite this article as: Tobin, T.S., et al., Modeling climatic effects of carbon dioxide emissions from Deccan Traps Volcanic Eruptions around the Cretaceous–Paleogene boundar..., Palaeogeogr. Palaeoclimatol. Palaeoecol. (2016), http://dx.doi.org/10.1016/j.palaeo.2016.05.028

4.2.4. Duration of eruptive sequence

The duration of the eruptive sequence for the Deccan Traps is poorly constrained. Recent work (Renne et al., 2015; Richards et al., 2015; Schoene et al., 2015) suggest that a vast majority of the eruptive sequence is constrained within C29R, limiting the eruption to approximately 730 ka, though some of the upper Mahabelshwar flows are C29N. Further constraint using the K–Pg boundary is possible, but the placement of this boundary within the Deccan sequence is contested (Renne et al., 2015; Schoene et al., 2015). Additionally, the duration of C29R has recently been proposed as substantially shorter, approximately 345 ka (Sprain et al., 2015), which would compress the time available for Deccan Traps eruptions. Given the uncertainty, we tested a range of possibilities for eruptive sequence duration, from 250 ka to 850 ka (Fig. 9). Eruptive sequence duration does affect peak CO_2 level and air temperature, though the effect is non-linear. We tested the climate effects of eruptive sequence duration while holding total CO_2 emission constant by reducing the spacing between equal size and length eruptions. A more than threefold (250 to 850 ka) increase in duration results in only a 40% reduction in temperature change (+1.6 ° C to +0.95 °C).

4.2.5. Total CO_2

Estimates for total CO_2 released from the Deccan Traps eruptive sequence are primarily determined by estimations of the original total volume of lava. The volatile content of the lava is also important, but most studies have adopted the estimates from Self et al. (2006) of 0.5% by weight volatile release, or 14 Tg of CO_2 released per 1 km^3 of basalt, allowing for estimation of total CO_2 release based on basalt volume. Total eruptive volumes are commonly reconstructed as between 0.7×10^6 km^3 and 2.5×10^6 km^3 (Self et al., 2006; Chenet et al., 2009; Bond and Wignall, 2014) though values as high as 4×10^6 km^3 have been reported (Courtillot and Renne, 2003). We tested a variety of total emitted CO_2 amounts over almost a full order of magnitude ranging from 2.4×10^{17} to 1.8×10^{18} mol of CO_2. We tested each value under the following parameters: total eruptive sequence — 400 ka; number of eruptions — 20; length of individual eruptions — 5 ka; periodic, equal-sized eruptions (EP1 — above). The length and number of individual eruptions are unrealistic, but were chosen for visual clarity, since testing of these parameters reveals that they are largely unimportant. Table 1 summarizes the various CO_2 emission estimates, sources, and peak temperatures and pCO_2 (measured immediately after final eruption). Unsurprisingly, the amount of CO_2 emitted is the primary control on peak temperature and CO_2 levels (Fig. 10), and thus the most important to understand for potential biological implications, though eruptive duration and pattern provide additional important constraints. The published range of volume estimates (Table 1) could be compatible with temperature increases from less than 1 °C up to 6 °C.

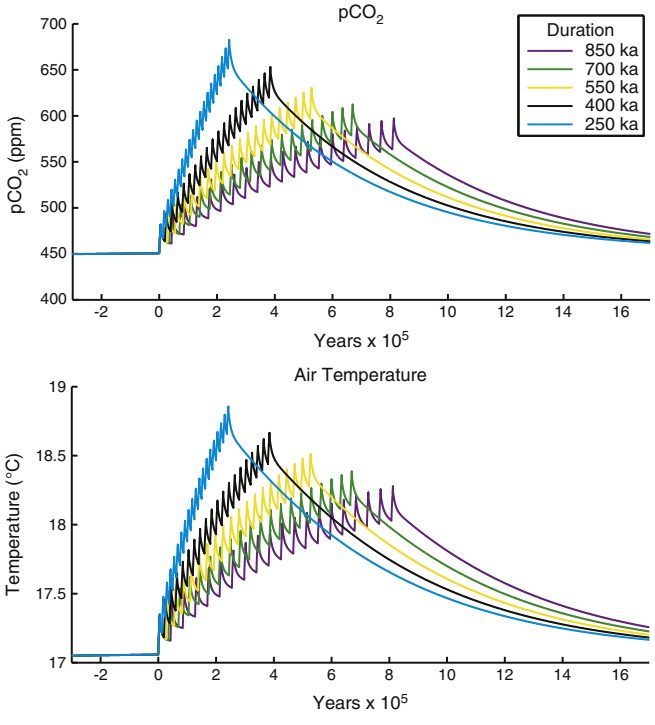

Fig. 9. Test of the effects of varying the duration of the overall Deccan eruptive sequence. Shorter eruptive durations lead to higher peak pCO2 and temperature values.

5. Plausibility of Deccan Traps — warming link

It is clear that the primary variables controlling the magnitude of any Deccan associated warming are the total CO_2 emitted and the duration and pattern of the eruptive sequence. Fig. 11 shows the model result using 4.14×10^{17} mol of CO_2 and an eruptive duration of 400 ka, which are likely the best available estimates from the literature (see Section 4.2). In this scenario peak temperatures rise 1.5 °C above background after 400 ka and remain at least 0.5 °C above initial conditions for more than 800 ka after the eruptive sequence ceases. For the upper range of plausible total CO_2 emission estimates, it appears that measurable global warming is possible due to Deccan Traps volcanism. The magnitude of this response does vary if we modify the climate sensitivity used in this model (3 °C per CO_2 doubling), but the changes in peak temperature at different climate sensitivities are very close (though not exact) to the values expected by the proportional differences in climate sensitivity (Fig. 12), which allows other model results above and below to be approximated for other climate sensitivities.

5.1. Comparisons with proxy records

A global 1.5 °C increase in temperatures is sufficiently large to leave an identifiable signal in most locations with most paleotemperature proxies, but the magnification of temperature change in polar regions, leading to ~3.0 °C increase (Holland and Bitz, 2003), could be easier to recognize. A warming of (3–6 °C) has been identified in the Cretaceous portion of C29R, though in most reconstructions temperatures return to background levels before the K–Pg boundary (Li and Keller, 1998; Barrera and Savin, 1999; Wilf et al., 2003). Many records have gaps at the K–Pg boundary because they are derived from ocean cores with insufficient foraminifera abundance in the earliest Paleogene for $\delta^{18}O$ analysis. A high-latitude continuous molluscan $\delta^{18}O$ temperature record across the K–Pg boundary (Tobin et al., 2012) showed a single warming event crossing the K–Pg boundary, though the data could plausibly be interpreted as separate pre- and post- boundary pulses. Another record from the northern hemisphere mid-latitudes, found cooling over the Cretaceous C29R interval (Tobin et al., 2014).

We attempted to match some of the paleoclimate estimates by adjusting the CO_2 emission parameters within the bounds discussed above. The warming event recorded by Tobin et al. (2012) had a peak magnitude of +7 °C at a paleolatitude of 62°S (roughly equivalent to +3.5 °C global average) and duration of 800 ka before return to near background temperatures (within 0.5 °C), though this period would be revised to ~400 ka if new C29R durations of Sprain et al. (2015) are used. This magnitude of global warming can be achieved with total CO_2 emissions towards the high end of published estimates, between 7.5 and 8.0×10^{17} mol, for eruptive sequence durations between about 100–600 ka. However, the warming duration of Tobin et al. (2012) is shorter than the persistence of elevated temperature (>0.5 °C above background) in all model runs with the standard parameters used to control CO_2 draw down.

Please cite this article as: Tobin, T.S., et al., Modeling climatic effects of carbon dioxide emissions from Deccan Traps Volcanic Eruptions around the Cretaceous–Paleogene boundar..., Palaeogeogr. Palaeoclimatol. Palaeoecol. (2016), http://dx.doi.org/10.1016/j.palaeo.2016.05.028

Table 1
Summary of different published estimates for Deccan Traps volume and subsequent CO_2 emissions, and their modeled climatic effects.

Source	Lava volume ($\times 10^6$ km^3)	Total CO_2 ($\times 10^{17}$ moles)	Peak CO_2 (ppm)	Peak temperature (°C)
Self et al. (2006)	0.7	2.39	547 (+97)	17.9 (+0.8)
Jay and Widdowson (2008)	1.3	4.14	627 (+177)	18.5 (+1.4)
Self et al. (2006)	2	6.36	740 (+290)	19.2 (+2.1)
Chenet et al. (2009)	2.5	7.95	831 (+381)	19.7 (+2.6)
Javoy and Michard (1989)	??	18	1589 (+1149)	22.5 (+5.4)

5.2. Enhanced silicate weathering

In order for the model to match any of the proxy records of near K–Pg warming, it is necessary for CO_2 to be drawn down at a faster rate during and/or after the eruptive sequence than previous studies using the GEOCARB based model. Given the creation of large areas of basalt in subtropical latitudes, it is likely that silicate weathering rates increased during and after the Deccan Traps eruptive sequence, increasing CO_2 drawdown rates over this period. Dessert et al. (2001) find that weathering of the Deccan Traps basalt province is responsible for 5% of modern day global silicate weathering, and it is reasonable to propose that this contribution was higher shortly after the eruptive sequence.

We modified the model to allow increased rates of silicate weathering during and after the eruption to see if these conditions resulted in temperature changes that more closely match proxy records. This modification was the simple inclusion of a multiplying factor to the equation governing the rate of CO_2 drawdown from silicate weathering. A full discussion of the factors controlling the CO_2–weathering relationship in this model is found in Berner and Kothavala (2001) and references therein. We found a good fit to the magnitude of paleotemperature change from Tobin et al. (2012) with a total emission of 10 x 10^{17} mol of CO_2 over 350 ka and the EP3 eruption pattern. We increased the strength of silicate weathering by 5% for 1050 ka from the start of the eruption to replicate the increased weathering of the Deccan Traps, and were able to achieve a 3.3 °C warming at peak that was reduced to 0.5 °C over an 800 ka period starting 100 ka after the initiation of the eruptions (Fig. 13 — purple line), a reasonable correspondence with Tobin et al. (2012) given polar amplification. For the potentially constrained timeline implied by the C29R durations from Sprain et al. (2015), we would need to induce a global 3–3.5 °C warming at peak that is reduced to 0.5 °C over a ~400 ka period. This response was achieved under the same eruption scenarios as above, but with the eruptive sequence duration restricted to 200 ka, and silicate weathering intensity increased by 13% (Fig. 13 — green line). This period is also comparable to the warming duration found by Li and Keller (1998), data which are also plotted in Fig. 12.

Both of the enhanced weathering scenarios assume that weathering rates could not increase from syn-eruptive conditions into the post eruptive sequence, and if we remove this restriction it becomes easier to match paleotemperature records. Fig. 13 (yellow line) shows results when eruptive sequence duration is expanded to 400 ka, and total CO_2 emissions of 8.0 × 10^{17} mol, but silicate weathering is increased (20%) only during the 300 ka following the eruption. A warming event of 2.5–3 °C can be generated that lasts about 500 ka. This artificial modification allows CO_2 to accumulate during the eruption and then be drawn down quickly post eruption, which appears necessary to fully match proxy records. This scenario is somewhat unrealistic, both in terms of the magnitude of warming and the timing of onset for increased weathering.

These comparisons indicate that the Deccan Traps volcanism is a potential candidate for causing warming around the K–Pg boundary, given

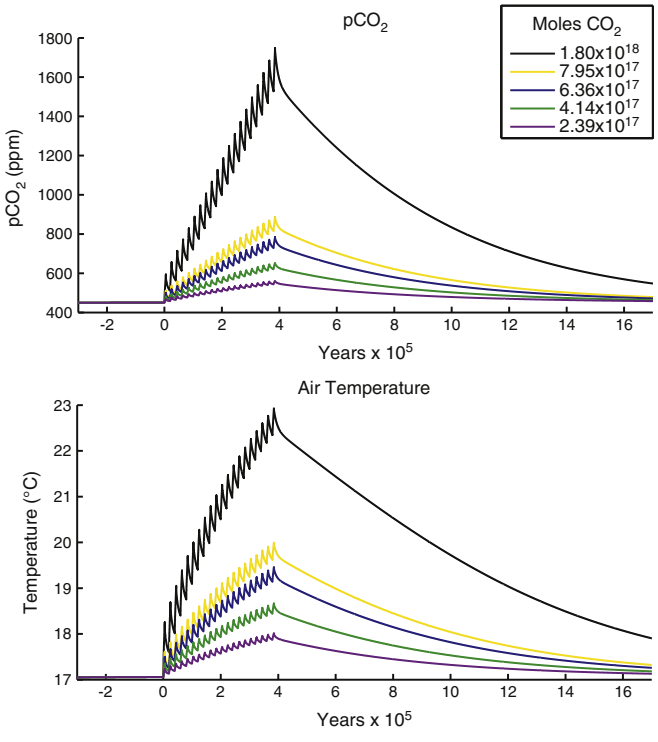

Fig. 10. Test of the effects of varying the total emitted CO_2 from the Deccan sequence. This value has the strongest control on model results.

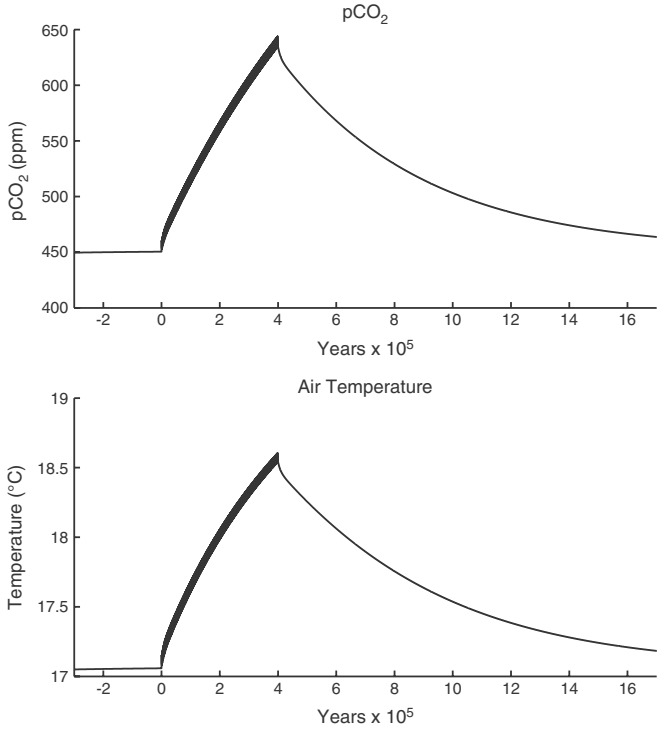

Fig. 11. Model simulation using the most recent published estimates for total eruptive CO_2 (4.14×10^{17} mol), eruptive duration (400 ka), and using reasonable estimates of total number (250) and length (20 years) of eruptions (see text).

Please cite this article as: Tobin, T.S., et al., Modeling climatic effects of carbon dioxide emissions from Deccan Traps Volcanic Eruptions around the Cretaceous–Paleogene boundar..., Palaeogeogr. Palaeoclimatol. Palaeoecol. (2016), http://dx.doi.org/10.1016/j.palaeo.2016.05.028

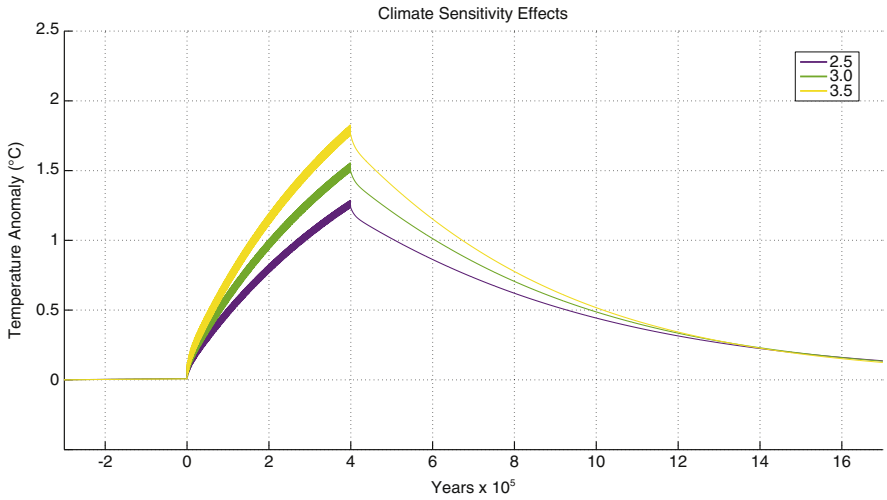

Fig. 12. Effects of altering climate sensitivity on peak temperature anomalies. Peak temperature difference is very close to proportional difference in climate sensitivity.

the published estimates of total CO_2 emissions. The main discrepancy between proxies and the model may not be the magnitude of warming, but in the rate of return to a pre-eruption climate, which appears to occur faster than the model can simulate without artificial alteration of weathering rates. There may be complexity in this process that is not well simulated with this simple model. Better constraints on the total amount, duration, and patterns of CO_2 release will allow us to better test this hypothesis, as there are many proposed Deccan emission scenarios that are incapable of generating the paleotemperature patterns observed. If the Deccan eruptions did not create the warming pulse at K–Pg boundary though, another candidate must be identified.

6. Conclusion

The results presented above add to the literature exploring possible links between flood basalt volcanism and mass extinction, though much work remains to be completed. Previous modeling attempts have treated Deccan volcanism as a single ongoing eruption (Caldeira and Rampino, 1990a; Caldeira and Rampino, 1990b), and while our results suggest that this is a reasonable approach, there are additional complexities in the timing and pattern of eruptions that contribute to the overall climate response. Additionally, we model more recent estimates of emitted CO_2, which are larger than many of the volumes considered by Caldeira and Rampino. Our attempts to match proxy data indicating a roughly 3 °C global temperature increase during this period show a plausible correspondence in terms of volume and timing, but require CO_2 emissions near the larger end of published estimates in combination with increased weathering rates. A 3 °C warming over several 100 ka may be sufficient to contribute to the K–Pg mass extinction, though probably not as a direct kill mechanism. Rather, if warming does contribute to the mass extinction in most locations it is likely to do so through some form of "press-pulse" mechanism, in which warming stresses ecosystems, which then respond more catastrophically to the Chicxulub impactor (Arens and West, 2008; Mitchell et al.,

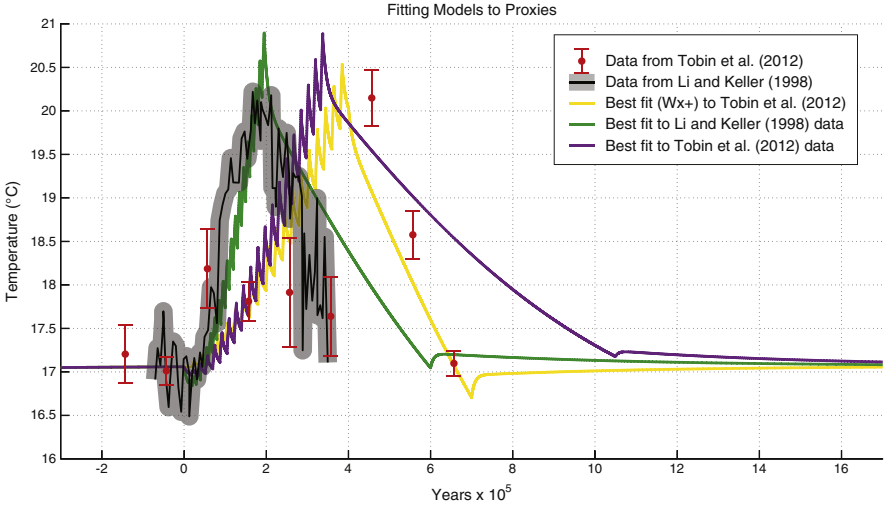

Fig. 13. Compilation of model simulations created to conform to proxy data. Temperature data from Tobin et al. (2012) has been shifted to match baselines with the modeled global temperatures (+10 °C) and the magnitude of changes have been halved to reflect the effects of polar amplification (see text). Temperature data from Li and Keller (1998) has also been shifted to match model baselines (+7 °C), and the time scale compressed to reflect more recent estimates of the length of the Cretaceous portion of magnetochron C29R. Gray window indicates approximate error (not shown in original source). Purple line — fit to Tobin et al. (2012) data: total emitted CO_2 — 1×10^{18} mol, emitted using the EP3 pattern, eruptive duration — 350 ka. Silicate weathering was increased by 5% during the eruption and for another 700 ka post eruption. Green line — fit to short duration of Tobin et al. (2012) or duration/magnitude from Li and Keller (1998) data: total emitted CO_2 — 1×10^{18} mol, emitted using the EP3 pattern, eruptive duration - 200 ka. Silicate weathering was increased by 13% during the eruption and for another 400 ka post eruption. Yellow line — fit to Tobin et al. (2012) temperature data with enhanced silicate weathering (+20%) beginning after the eruptive sequence: total CO_2 emitted — 8×10^{17} mol, emitted using the EP3 pattern, eruptive duration — 400 ka. (For interpretation of the references to color in this figure legend, the reader is referred to the web version of this article.)

Please cite this article as: Tobin, T.S., et al., Modeling climatic effects of carbon dioxide emissions from Deccan Traps Volcanic Eruptions around the Cretaceous–Paleogene boundar..., Palaeogeogr. Palaeoclimatol. Palaeoecol. (2016), http://dx.doi.org/10.1016/j.palaeo.2016.05.028

2012; Arens et al., 2014). It is also possible that sudden short-term cooling from SO_2 emissions is the primary contribution of Deccan eruptions to the biological catastrophe (Bond and Wignall, 2014; Mussard et al., 2014) though we do not address these effects in our model. A variety of studies (Tobin et al., 2012; Archibald, 2014; Keller, 2014; Tobin et al., 2014; Wilson, 2014; Wilson et al., 2014) suggest that there is destabilization of biotic communities over the Cretaceous portion of C29R, but at present a clear causal link with either short-term cooling or long-term warming has not been established. It is possible that the warming pulse near the K–Pg boundary could be Deccan-related, but entirely coincidental to the extinction.

Despite assertions of a consensus (Schulte et al., 2010), there is still vigorous debate over the potential contribution of Deccan Traps volcanism to the end Cretaceous mass extinction (Archibald et al., 2010; Courtillot and Fluteau, 2010; Keller et al., 2010). Recent geochronological work (Renne et al., 2015; Richards et al., 2015) suggests that the majority of the Deccan sequence was erupted after the K–Pg boundary, which would render the traps an unlikely candidate to contribute to the extinction; however further age constraints in the middle of the sequence are necessary. For the Deccan Traps to have contributed to the extinction they most likely did so through a combination of SO_2 driven cooling or CO_2 driven warming, but better understanding of the volcanic province is necessary to determine whether either or both of these factors are capable of biologically problematic climate change. Both Schmidt et al. (2016) and Mussard et al. (2014) demonstrate that significant cooling events driven by the Deccan Traps are possible. Here we demonstrate that CO_2 release is sufficient to drive substantial warming, and that the total amount, pattern, and duration of CO_2 emissions are the most important controls on the rate and magnitude of warming. Given published estimates of these values, the Deccan Traps are plausibly large enough to drive the warming observed in paleoclimate proxies, though the match with paleoclimate proxies required increased rates of weathering. We hope to revisit this model in the future as new estimates of size, timing, and pattern of the Deccan Traps eruptive sequence are generated.

Acknowledgements

The authors would like to acknowledge the assistance of the University of Washington Astrobiology Program which provided funding assistance for a graduate research rotation (IGERT - DGE-0504219AM04). Support of CMB from NASA Astrobiology Institute's Virtual Planetary Laboratory under Cooperative Agreement number NNA13AA93A. We also acknowledge two anonymous reviewers for their suggestions which improved the manuscript.

Appendix A. Supplementary data

Supplementary data to this article can be found online at http://dx.doi.org/10.1016/j.palaeo.2016.05.028.

References

Archer, D., Eby, M., Brovkin, V., Ridgwell, A., Cao, L., Mikolajewicz, U., Caldeira, K., Matsumoto, K., Munhoven, G., Montenegro, A., Tokos, K., 2009. Atmospheric lifetime of fossil fuel carbon dioxide. Annu. Rev. Earth Planet. Sci. 37, 117–134.
Archibald, J.D., 2014. What the dinosaur record says about extinction scenarios. Geol. Soc. Am. Spec. Pap. 505, 213–224.
Archibald, J.D., Clemens, W.A., Padian, K., Rowe, T., Macleod, N., Barrett, P.M., Gale, A., Holroyd, P., Sues, H.D., Arens, N.C., Horner, J.R., Wilson, G.P., Goodwin, M.B., Brochu, C.A., et al., 2010. Cretaceous extinctions: multiple causes. Science 328 (5981), 973.
Arens, N.C., West, I.D., 2008. Press-pulse: a general theory of mass extinction? Paleobiology 34 (4), 456–471. http://dx.doi.org/10.1666/07034.1.
Arens, N.C., Thompson, A., Jahren, A.H., 2014. A Preliminary Test of the Press-Pulse Extinction Hypothesis: Palynological Indicators of Vegetation Change Preceding the Cretaceous-Paleogene Boundary, McCone County, Montana, USA, in Geological Society of America Special Papers, Geological Society of America. pp. 209–227.
Barrera, E., Savin, S.M., 1999. Evolution of late Campanian-Maastrichtian marine climates and oceans. Geol. Soc. Am. Spec. Pap. 332, 245–282.
Beerling, D.J., Royer, D.L., 2011. Convergent Cenozoic CO2 history. Nat. Geosci. 4, 418–420.
Beerling, D.J., Lomax, B.H., Royer, D.L., Upchurch, G.R., Kump, L.R., 2002. An atmospheric pCO2 reconstruction across the Cretaceous-Tertiary boundary from leaf megafossils. Proc. Nat. Acad. Sci. US Am. 99 (12), 7836.
Beerling, D.J., Fox, A., Anderson, C.W., 2009. Quantitative uncertainty analyses of ancient atmospheric CO2 estimates from fossil leaves. Am. J. Sci. 309 (9), 775–787.
Berner, R.A., 1994. GEOCARB II; a revised model of atmospheric CO 2 over Phanerozoic time. Am. J. Sci. 294 (1), 56.
Berner, R.A., Kothavala, Z., 2001. GEOCARB III: A revised model of atmospheric CO2 over Phanerozoic time. Am. J. Sci. 301 (2), 182–204.
Blakey, R., 2012. Paleogeography of North America: Plateau Geosystems Inc.
Bond, D.P., Wignall, P.B., 2014. Large igneous provinces and mass extinctions: an update. Geol. Soc. Am. Spec. Pap. 505, SPE505-02.
Breecker, D.O., Sharp, Z.D., McFadden, L.D., 2010. Atmospheric CO2 concentrations during ancient greenhouse climates were similar to those predicted for A.D. 2100. Proc. Natl. Acad. Sci. 107 (2), 576–580. http://dx.doi.org/10.1073/pnas.0902323106.
Caldeira, K.G., Rampino, M.R., 1990a. Carbon dioxide emissions from Deccan volcanism and a K/T boundary greenhouse effect. Geophys. Res. Lett. 17 (9), 1299–1302.
Caldeira, K.G., Rampino, M.R., 1990b. Deccan volcanism, greenhouse warming, and the Cretaceous/Tertiary boundary. Geol. Soc. Am. Spec. Pap. 247, 117–123.
Chenet, A.L., Quidelleur, X., Fluteau, F., Courtillot, V., Bajpai, S., 2007. 40K-40Ar dating of the Main Deccan large igneous province: further evidence of KTB age and short duration. Earth Planet. Sci. Lett. 263 (1–2), 1–15.
Chenet, A.L., Fluteau, F., Courtillot, V.E., Gerard, M., Subbarao, K.V., 2008. Determination of rapid Deccan eruptions across the Cretaceous-Tertiary boundary using paleomagnetic secular varation: results from a 1200-m-thick section in the Mahabaleshwar escarpment. J. Geophys. Res. 113.
Chenet, A.L., Courtillot, V., Fluteau, F., Gérard, M., Quidelleur, X., Khadri, S.F.R., Subbarao, K.V., Thordarson, T., 2009. Determination of rapid Deccan eruptions across the Cretaceous-Tertiary boundary using paleomagnetic secular variation: 2. Constraints from analysis of eight new sections and synthesis for a 3500-m-thick composite section. J. Geophys. Res. 114, B06103.
Courtillot, V.E., Fluteau, F., 2010. Cretacous extinctions: the volcanic hypothesis. Science 328, 973–974.
Courtillot, V.E., Renne, P.R., 2003. On the ages of flood basalt events. Geodynamics 335, 113–140.
Dessert, C., Dupré, B., François, L.M., Schott, J., Gaillardet, J., Chakrapani, G., Bajpai, S., 2001. Erosion of Deccan Traps determined by river geochemistry: impact on the global climate and the ^{87}Sr ^{86}Sr ratio of seawater. Earth Planet. Sci. Lett. 188 (3), 459–474.
Feulner, G., 2012. The faint young Sun problem. Rev. Geophys. 50 (2). http://dx.doi.org/10.1029/2011RG000375.
Font, E., Fabre, S., Nédélec, A., Adatte, T., Keller, G., Veiga-Pires, C., Ponte, J., Mirão, J., Khozyem, H., Spangenberg, J.E., 2014. Atmospheric halogen and acid rains during the main phase of Deccan eruptions: magnetic and mineral evidence. Geol. Soc. Am. Spec. Pap. 505, SPE505-18.
Holland, M.M., Bitz, C.M., 2003. Polar amplification of climate change in coupled models. Clim. Dyn. 21 (3–4), 221–232. http://dx.doi.org/10.1007/s00382-003-0332-6.
Javoy, M., Michard, G., 1989. Global catastrophes and volcanic events: a comparison of volcanic and industrial outgassings under normal and catastrophic conditions. AGU EOS Trans 70, 1421.
Jay, A.E., Widdowson, M., 2008. Stratigraphy, structure and volcanology of the SE Deccan continental flood basalt province: implications for eruptive extent and volumes. J. Geol. Soc. 165 (1), 177–188. http://dx.doi.org/10.1144/0016-76492006-062.
Jay, A.E., Niocaill, C.M., Widdowson, M., Self, S., Turner, W., 2009. New palaeomagnetic data from the Mahabaleshwar Plateau, Deccan Flood Basalt Province, India: implications for the volcanostratigraphic architecture of continental flood basalt provinces. J. Geol. Soc. 166 (1), 13–24. http://dx.doi.org/10.1144/0016-76492007-150.
Keller, G., 2014. Deccan volcanism, the Chicxulub impact, and the end-Cretaceous mass extinction: coincidence? Cause and effect? Geol. Soc. Am. Spec.Pap., 505, 57–89.
Keller, G., Adatte, T., Pardo, A., Bajpai, S., Khosla, A., Samant, B., 2010. Cretaceous extinctions: evidence overlooked. Science 328, 974–975.
Li, L., Keller, G., 1998. Abrupt deep-sea warming at the end of the Cretaceous. Geology 26 (11), 995–998.
MacLeod, K.G., Huber, B.T., Isaza-Londoño, C., 2005. North Atlantic warming during global cooling at the end of the Cretaceous. Geology 33 (6), 437. http://dx.doi.org/10.1130/G21466.1.
Mitchell, J.S., Roopnarine, P.D., Angielczyk, K.D., 2012. Late Cretaceous restructuring of terrestrial communities facilitated the end-Cretaceous mass extinction in North America. Proc. Nat. Acad. Sci. 109 (46), 18857–18861.
Molina, E., Alegret, L., Arenillas, I., Arz, J.A., Gallala, N., Hardenbol, J., Salis, K., Steurbaut, E., Vandenberghe, N., Zaghbib-Turki, D., 2006. The Global Boundary Stratotype Section and Point for the base of the Danian Stage (Paleocene, Paleogene," Tertiary", Cenozoic) at El Kef, Tunisia-Original definition and revision. Episodes 29 (4), 263.
Mussard, M., Le Hir, G., Fluteau, F., Lefebvre, V., Goddéris, Y., 2014. Modeling the carbon-sulfate interplays in climate changes related to the emplacement of continental flood basalts. Geol. Soc. Am. Spec. Pap. 505, 339–352.
Ogg, J.G., 2012. Geomagnetic Polarity Time Scale, in The Geologic Time Scale. Elsevier, pp. 85–113.
Renne, P.R., Sprain, C.J., Richards, M.A., Self, S., Vanderkluysen, L., Pande, K., 2015. State shift in Deccan volcanism at the Cretaceous-Paleogene boundary, possibly induced by impact. Science 350 (6256), 76–78.
Richards, M.A., Alvarez, W., Self, S., Karlstrom, L., Renne, P.R., Manga, M., Sprain, C.J., Smit, J., Vanderkluysen, L., Gibson, S.A., 2015. Triggering of the largest Deccan eruptions by the Chicxulub impact. Geol. Soc. Am. Bull. http://dx.doi.org/10.1130/B31167.1.
Royer, D.L., 2003. Estimating latest Cretaceous and Tertiary atmospheric CO_2 from stomatal indices. Spec. Pap.-Geol. Soc. Am. 79–94.

Please cite this article as: Tobin, T.S., et al., Modeling climatic effects of carbon dioxide emissions from Deccan Traps Volcanic Eruptions around the Cretaceous–Paleogene boundar..., Palaeogeogr. Palaeoclimatol. Palaeoecol. (2016), http://dx.doi.org/10.1016/j.palaeo.2016.05.028

Royer, D.L., 2010. Fossil soils constrain ancient climate sensitivity. Proc. Natl. Acad. Sci. 107 (2), 517–518. http://dx.doi.org/10.1073/pnas.0913188107.

Schmidt, A., Skeffington, R.A., Thordarson, T., Self, S., Forster, P.M., Rap, A., Ridgwell, A., Fowler, D., Wilson, M., Mann, G.W., Wignall, P.B., Carslaw, K.S., 2016. Selective environmental stress from sulphur emitted by continental flood basalt eruptions. Nat. Geosci. http://dx.doi.org/10.1038/ngeo2588.

Schoene, B., Samperton, K.M., Eddy, M.P., Keller, G., Adatte, T., Bowring, S.A., Khadri, S.F., Gertsch, B., 2015. U-Pb geochronology of the Deccan Traps and relation to the end-Cretaceous mass extinction. Science 347 (6218), 182–184.

Schulte, P., Alegret, L., Arenillas, I., Arz, J.A., Barton, P.J., Bown, P.R., Bralower, T.J., Christeson, G.L., Claeys, P., Cockell, C.S., Collins, G.S., Deutsch, A., Goldin, T.J., Goto, K., et al., 2010. The Chicxulub asteroid impact and mass extinction at the Cretaceous-Paleogene boundary. Science 327 (5970), 1214–1218. http://dx.doi.org/10.1126/science.1177265.

Self, S., Widdowson, M., Thordarson, T., Jay, A.E., 2006. Volatile fluxes during flood basalt eruptions and potential effects on the global environment: A Deccan perspective. Earth Planet. Sci. Lett. 248 (1), 518–532.

Self, S., Schmidt, A., Mather, T.A., 2014. Emplacement characteristics, time scales, and volcanic gas release rates of continental flood basalt eruptions on Earth. Geol. Soc. Am. Spec. Pap. 505, SPE505–SPE516.

Self, S., Glaze, L.S., Schmidt, A., Mather, T.A., 2015. Volatile Release From Flood Basalt Eruptions: Understanding the Potential Environmental Effects, in Volcanism and Global Environmental Change. Cambridge University Press, pp. 164–176.

Seton, M., Gaina, C., Müller, R.D., Heine, C., 2009. Mid-Cretaceous seafloor spreading pulse: fact or fiction? Geology 37 (8), 687–690.

Sprain, C.J., Renne, P.R., Wilson, G.P., Clemens, W.A., 2015. High-resolution chronostratigraphy of the terrestrial Cretaceous-Paleogene transition and recovery interval in the Hell Creek region, Montana. Geol. Soc. Am. Bull. 127 (3–4), 393–409. http://dx.doi.org/10.1130/B31076.1.

Tobin, T.S., Ward, P.D., Steig, E.J., Olivero, E.B., Hilburn, I.A., Mitchell, R.N., Diamond, M.R., Raub, T.D., Kirschvink, J.L., 2012. Extinction patterns, δ18O trends, and magnetostratigraphy from a southern high-latitude Cretaceous–Paleogene section: Links with Deccan volcanism. Palaeogeogr., Palaeoclimatol., Palaeoecol. 350–352, 180–188. http://dx.doi.org/10.1016/j.palaeo.2012.06.029.

Tobin, T.S., Wilson, G.P., Eiler, J.M., Hartman, J.H., 2014. Environmental change across a terrestrial Cretaceous-Paleogene boundary section in eastern Montana, USA, constrained by carbonate clumped isotope paleothermometry. Geology 42 (4), 351–354. http://dx.doi.org/10.1130/G35262.1.

Wilf, P., Johnson, K.R., Huber, B.T., 2003. Correlated terrestrial and marine evidence for global climate changes before mass extinction at the Cretaceous–Paleogene boundary. Proc. Nat. Acad. Sci. US Am. 100 (2), 599–604.

Wilson, G.P., 2014. Mammalian extinction, survival, and recovery dynamics across the Cretaceous-Paleogene boundary in northeastern Montana, U.S.A. Geol. Soc. Am. Spec. Pap. 503, 365–390.

Wilson, G.P., DeMar, D., Carter, G., 2014. Extinction and survival of salamander and salamander-like amphibians across the Cretaceous-Paleogene boundary in northeastern Montana USA. Geol. Soc. Am. Spec. Pap. 503, 271–298.

Please cite this article as: Tobin, T.S., et al., Modeling climatic effects of carbon dioxide emissions from Deccan Traps Volcanic Eruptions around the Cretaceous–Paleogene boundar..., Palaeogeogr. Palaeoclimatol. Palaeoecol. (2016), http://dx.doi.org/10.1016/j.palaeo.2016.05.028